Journal of Solid State Chemistry 182 (2009) 2298–2306

Contents lists available at ScienceDirect

Journal of Solid State Chemistry

journal homepage: www.elsevier.com/locate/jssc

Novel symmetrical coralloid Cu 3D superstructures: Solid-state synthesis from a Cu-carboxylate MOF and their in-situ thermal conversion

Lingyun Chen [a,*], Yongming Shen [b], Junfeng Bai [b,*], Chunzhao Wang [c]

[a] College of Chemistry and Chemical Engineering, Chongqing University, Chongqing 400030, PR China
[b] State Key Laboratory of Coordination Chemistry, School of Chemistry and Chemical Engineering, Nanjing University, Nanjing 210093, PR China
[c] State Key Laboratory of Palaeobiology and Stratigraphy, Nanjing Institute of Geology and Palaeontology, Chinese Academy, Nanjing 210008, PR China

ARTICLE INFO

Article history:
Received 14 March 2009
Received in revised form
30 May 2009
Accepted 7 June 2009
Available online 13 June 2009

Keywords:
Metal-organic framework
Solid-state thermolysis
Superstructure
Cu
CuO

ABSTRACT

We describe here a one-step solid-state process for the synthesis of metal three-dimensional (3D) superstructures from a metal-organic framework (MOF). Novel symmetrical coralloid Cu 3D superstructures with surface interspersed with clusters of Cu nanoparticles were successfully synthesized by thermolysis of the $[Cu_3(btc)_2]$ (btc = benzene-1,3,5-tricarboxylato) MOF in a one-end closed horizontal tube furnace (OCTF). The obtained products were characterized by TGA, FT-IR, XRD, EDX, SEM, TEM, HRTEM and SAED. Different reaction conditions were discussed. Furthermore, the synthesized Cu samples were converted into CuO microstructures by in-situ calcination in the air. In addition, the possible formation mechanism was also proposed. This method is a simple and facile route, which builds a direct linkage between metal-carboxylate MOF crystals and metal nano- or microstructures and also opens a new application field of MOFs.

1. Introduction

Over the past decade, size- and morphology-controlled syntheses of materials at all dimensions from nanoscale to microscale have attracted a great deal of attention in the development of material technology and one of the challenges in material synthesis not only because of their unique size- and morphology-induced physical and chemical properties that differ greatly from their bulk counterparts, but also for their various potential applications in industry and technique areas [1–3]. Among these, inorganic materials attracted much attention owing to their special properties in optics, electronics, magnetic recording, catalysis, etc. [4–6]. And methods reported include vapor growth, solution-phase synthesis, and solid-state method and a variety of inorganic materials of metal, metal oxide, sulfide, hydrate, and other minerals with multiple structures of zero-dimensional (0D), 1D, 2D, and 3D structures and shapes of spheres, polyheda, rods, tubes, and slices have been successfully synthesized so far [7–10]. Up to date, rational synthesis of well-defined inorganic materials with uniform dimensions, size, and controlled shapes of architectures is of extraordinary importance in adjusting their chemical and physical properties because the electronic structure, bonding, surface energy, and chemical reactivity are directly related to their surface morphology. As a result, creation of novel superstructures of inorganic materials with special surface morphology and exploring of well-controlled methods for them is of high challenge and hot research topic [11].

In all the inorganic materials, metal and metal oxide nanostructures have received much attention because of their potential uses in a wide range of advanced applications [12,13]. Among various metallic and oxide materials, Cu and CuO are of particular interest because of their unique properties such as high electrical, catalytic and thermal conductivity of Cu [14,15] and semiconductor and powerful heterogeneous catalysts of CuO [16–18]. Furthermore, the properties of Cu and CuO are closely related to its microstructures, particularly its crystal size, orientation, and morphology. To date, a variety of Cu and CuO nano- and microstructures with various controlled sizes and shapes such as cubes, nanorods, cigar-shaped nanocrystals, and triangular nanocrystals, nanodisks, nanowires, and colloids with controlled shapes have been obtained by solid–vapor phase growth (SVG), microemulsion, and hydrothermal methods [19–23]. Up to now, exploration of simple and facile approaches for the fabrication of Cu and CuO is still of research attention and technique applications.

Meanwhile, recent years have witnessed rapid development of metal-organic frameworks (MOFs), one new kind of inorganic–organic hybrid species, not only due to their intriguing structures and unique properties, but also for their potential applications in catalysis, separation, sensors, and gas sorption or storage [24–28]. From the viewpoint of crystallology, utilization of inorganic–organic systems to generate metal oxide and semiconductors nano- and microstructures as well as films and hybrid

* Corresponding author.
E-mail addresses: lychen@cqu.edu.cn (L. Chen), bjunfeng@nju.edu.cn (J. Bai).

0022-4596/$ - see front matter Crown Copyright © 2008 Published by Elsevier Inc. All rights reserved.
doi:10.1016/j.jssc.2009.06.007

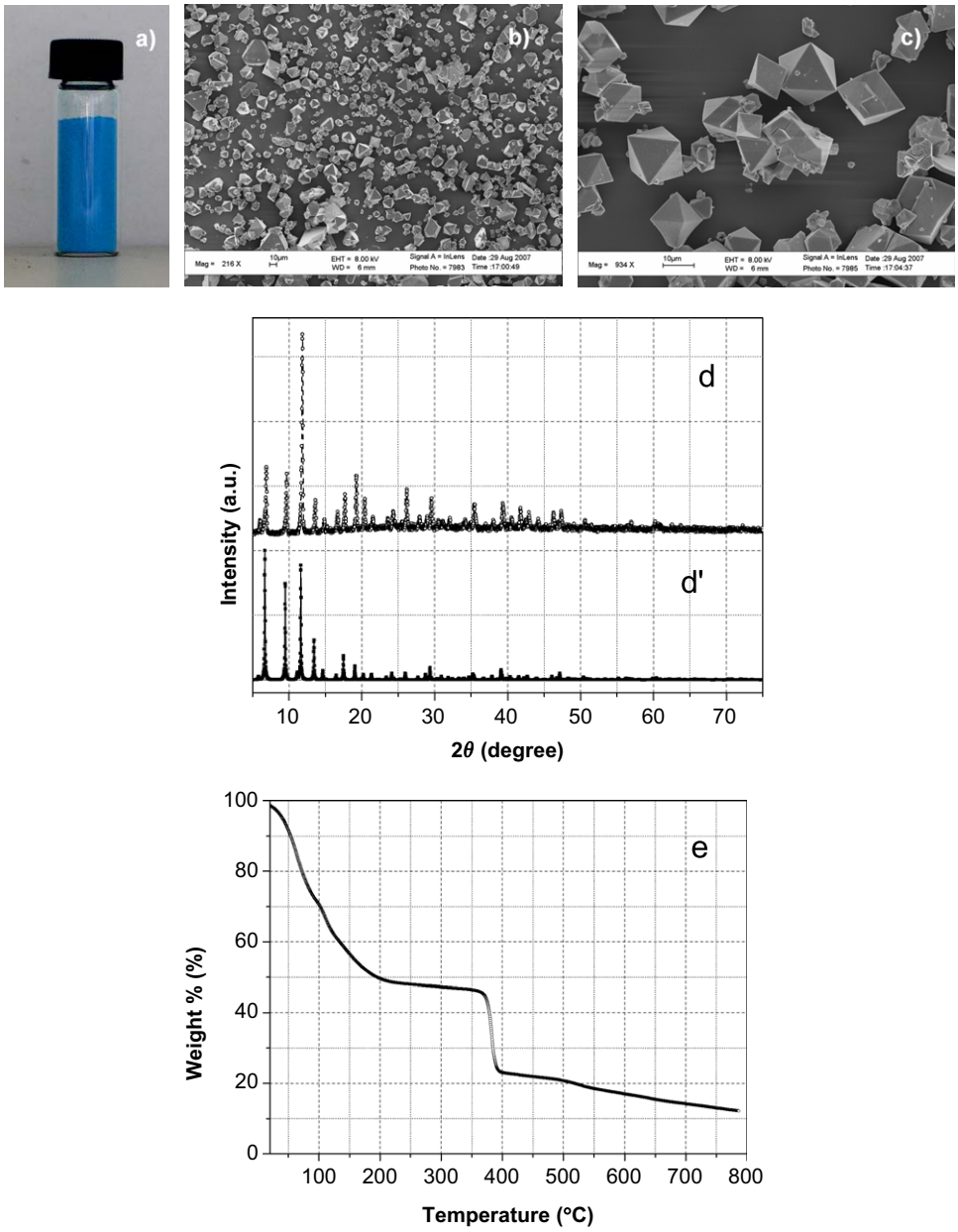

Fig. 1. (a) Photography, (b) and (c) different magnification FE-SEM images, (d) and (d′) experimental and stimulated XRD patterns, and (e) TGA curve with the heating rate of $10^{\circ}\,min^{-1}$ in a flowing N_2 atmosphere of as-synthesized Cu-*btc* MOF precursor microcrystals.

carboneous materials may be an affordable approach [29–33]. However, direct transformation of MOFs into metal nano- and microstructures is unexplored.

We are interested in the construction of coordination polymers (or MOFs) with high symmetrical and flexible ligands [34–37], and using novel coordination complexes which have unique compositions and structures to fabricate nano- and micromaterials with novel structures and properties [38,39]. For its unique structure and property, the $[Cu_3(btc)_2]$ (Cu-*btc*, *btc* = benzene-1,3,5-tricarboxylato) MOF has been widely investigated in gas separation and purification [40], catalytic activity [41], and hydrogen storage [42], as well as recently reported thin films [43]. However, little attention has been focused on solid-state synthesis of nano- and micromaterials from the Cu-*btc* MOF so far. In this paper, through thermolysis of the Cu-*btc* MOF in a one-end closed horizontal tube furnace (OCTF, see Experimental), we have been successfully realized the transformation of the Cu-*btc* into symmetrical coralloid Cu 3D microstructures with surface interspersed with clusters of Cu nanoparticles, which is a in-situ temperature-induced conversion without using any catalyst or template. Furthermore, in-situ calcination of above formed Cu superstructures resulted in CuO microstructures with superstructures retained. For the first time, one-step solid-state synthesis of Cu and CuO 3D superstructures was realized.

2. Experimental

2.1. Materials

All of the reagents were of analytical grade and used as received without any further purification. Deionized water was used throughout the experiments. Copper (II) nitrate trihydrate ($Cu(NO_3)_2 \cdot 3H_2O$) and absolute ethanol (C_2H_5OH) were purchased from Shanghai Chemical Co. Ltd., PR China. Benzene-1,3,5-tricarboxylic acid ($C_6H_3(COOH)_3$) was purchased from Alfa Aesar.

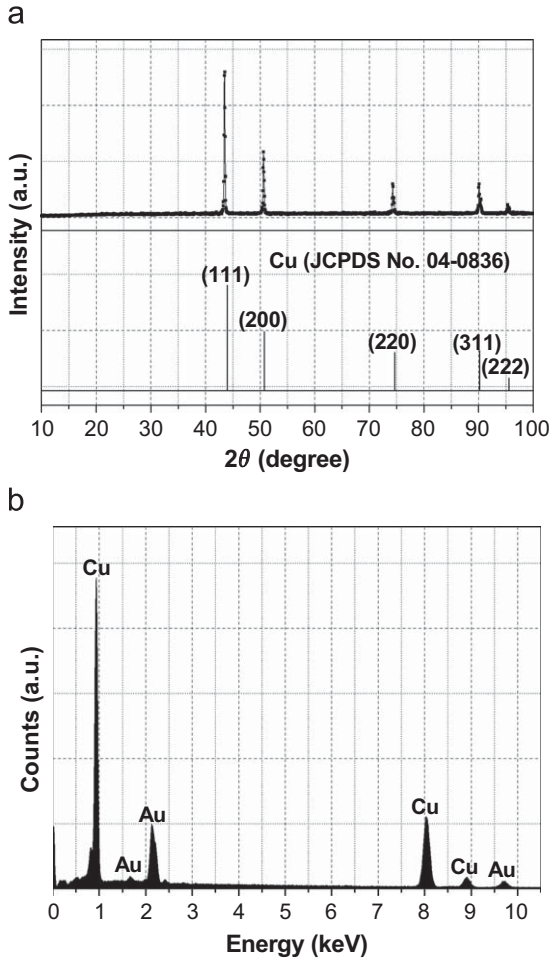

Fig. 2. (a) Typical XRD patterns and (b) EDX spectrum of as-synthesized products by thermolysis of the Cu-*btc* MOF in the OCTF at 500 °C for 10 h. The standard XRD data of Cu (JCPDS file No. 04-0836) are also presented in the figure for comparison.

2.2. Synthesis of the Cu-btc MOF microcrystals

The Cu-*btc* MOF microcrystals were synthesized by a modified method according to the literature [44]. In a typical synthesis, 0.22 g $Cu(NO_3)_2 \cdot 3H_2O$ (0.915 mmol) and 0.42 g H_3btc (2.025 mmol) were dissolved in a mixture solution of 3 ml H_2O and 9 ml absolute C_2H_5OH. After that, the resulting blue solution was stirred for 10 min and transferred into 15 ml Teflon, sealed, and hydrothermal treated at 120 °C for 6 h with the heating rate of 10 °C min After naturally cooling to room temperature, the solution was centrifuged, washed with absolute C_2H_5OH and water for several times and dried under vacuum for 5 h at room temperature.

2.3. Synthesis of Cu 3D superstructures from the Cu-btc MOF

All the synthesis reported here were carried out in a one-end sealed horizontal tube furnace, as reported elsewhere [38,39]. In a typical synthesis, the samples were obtained by the following method. Blue microcrystals of the precursor $[Cu_3(btc)_2]_n$ (about 0.2 g) were placed in a ceramic boat (with inside diameter of 0.6 cm and length of 5 cm). Firstly, a ceramic boat was positioned at the middle of a horizontal quartz tube (with inside diameter of 2 cm and length of 40 cm), along the axis with one-end closed and then the tube was mounted in the center of a conventional stainless steel tubular furnace. After that, the tube was heated at a rate of 10 °C min^{-1} to 500 °C for 10 h, and then kept at this temperature over the different course of time. After slow cooling to room temperature, red product was taken out, washed several times with distilled water and absolute ethanol, respectively, and finally dried in a vacuum at 60 °C for 5 h.

To see the reaction time effect, the same experiments were carried out at 500 °C for 5, 20, and 30 h.

2.4. In-situ conversion of Cu superstructures to CuO superstructures

Novel CuO superstructures were directly prepared from the above synthesized Cu products in Section 2.3. Conversion was carried out in above used horizontal tube furnace in Section 2.3 with both ends open at temperature of up to 500 °C for 10 h with a heating rate of 10 °C min^{-1}.

2.5. Direct calcination of the Cu-btc MOF into CuO

Direct calcination of the synthesized Cu-*btc* in the air was the same as the method in Section 2.4.

2.6. Characterization

Powder X-ray diffraction (XRD) patterns were collected in a Shimadzu XRD-6000 (operating at 40 kV and 30 mA) with graphite-monochromatized Cu*K*α radiation (wavelength $\lambda = 1.5148$ Å). Fourier transform infrared spectra (FT-IR) were obtained with Bruker VECTORTM 22 FTIR spectrometer at a resolution of 4 cm^{-1} with a Nic-Plan IR microscope. Thermogravimetric analysis (TGA) was carried out using a PerKinElmer Pyris 1 TGA (USA) with a heating rate of 10 °C min^{-1} in a flowing N_2 atmosphere. Field emission scanning electron microscopy (FE-SEM) studies were conducted with a well-aligned LEO1530VP SEM (Carl Zeiss INC.) operating at 200 kV and with an Oxford INCA energy dispersive X-ray analysis (EDX) to fulfill element microanalysis. Transmission electron microscopy (TEM) and selected-area electronic diffraction (SAED) studies were operated on a Philips TECNAI F20 S-TWIN TEM using an accelerating voltage of 120 kV and high resolution TEM (HRTEM) on a JEOL JSM-2100 TEM using an accelerating voltage of 200 kV. Sample grids were prepared by sonicating dry samples in ethanol for 15 min and depositing one drop of the suspension onto a carbon foil supported on a copper grid for TEM investigation.

3. Results and discussion

3.1. Preparation and characterization of the precursor Cu-MOF microcrystals

The Cu-*btc* MOF with high yield (see the sample photograph in Fig. 1(a)) was prepared under the hydrothermal condition, which resulted in the formation of large-scale blue microcrystals (see typical low magnification FE-SEM image in Fig. 1(b)). The high magnification FE-SEM image in Fig. 1(c) shows that as-synthesized Cu-*btc* microcrystals have an average diameter of about 10 μm. Fig. 1(d) and (d′) present powder X-ray diffraction patterns of the synthesized Cu-*btc* and its simulated result. All the *h k l* faces including (111), (200), (220), (311), (222), (400), (331), (420), (422), (333) and (400) of the formed Cu-*btc* MOF in the 2θ range of 5–20° match well with the reported result. The high diffraction peaks underlined the fact that the as-synthesized Cu-*btc* with its well defined peaks was well crystallized. EA [%] result calcd: C, 22.26; H, 5.75; Found: C, 22.2; H, 5.4. Furthermore, the FT-IR spectrum in Fig. S1 also demonstrates the surface structures of the synthesized Cu-*btc* MOF. All the above results

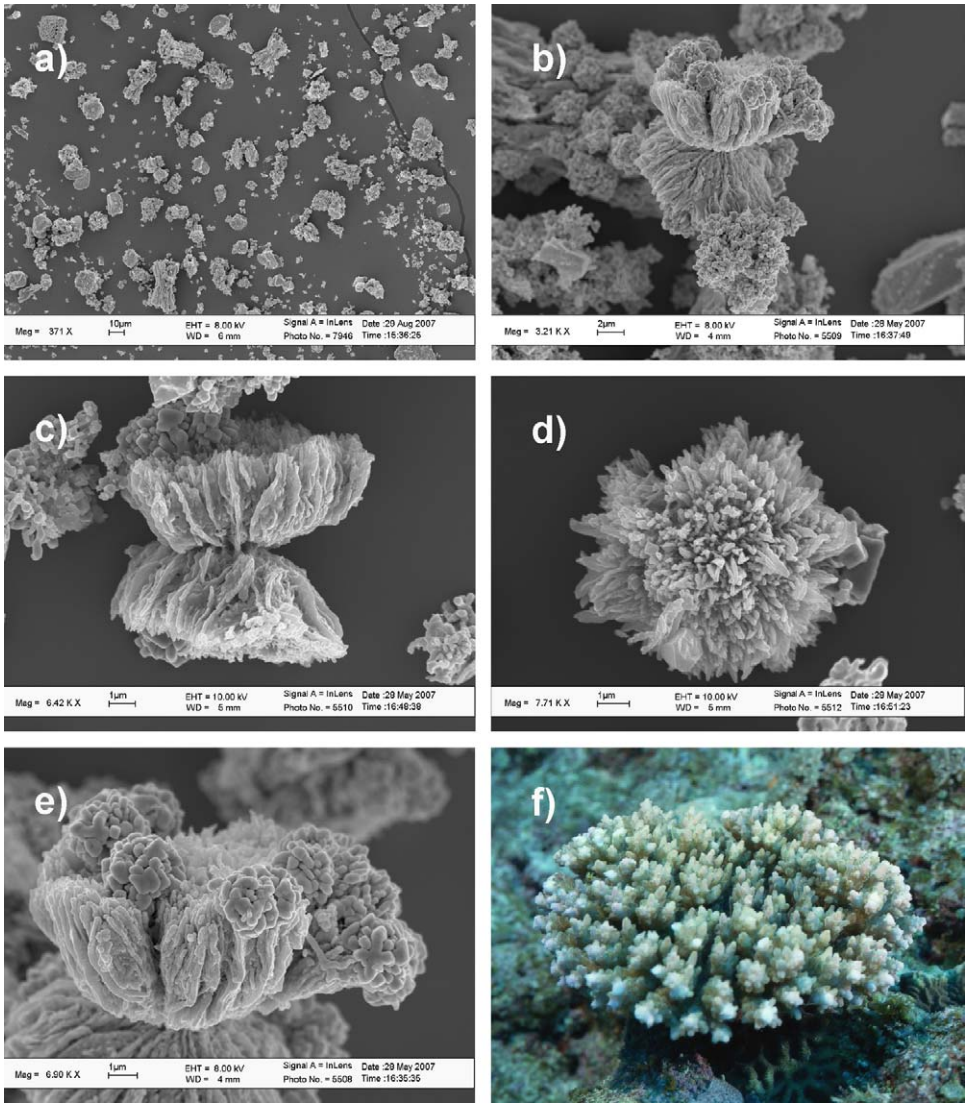

Fig. 3. (a), (b) Low- and (c)–(e) high magnification FE-SEM images of as-synthesized Cu superstructures by thermolsysis of the Cu-*btc* MOF in the OCTF at 500 °C for 10 h and (f) a photograph of one kind of corals.

indicate that the synthesized Cu-*btc* MOF matched well with the reported result in the literature. TGA was carried out in the interest of studying the thermal behavior of the as-synthesized Cu-*btc* MOF (in Fig. 1(e)). The experiment was performed on samples consisting of numerous single crystals of the Cu-*btc* under a N_2 atmosphere with a heating rate of 10 °C min^{-1}. As can be seen, the first major weight loss of ca. 53.5% corresponding to the departure of absorbed water molecules occurred in stages starting at 25 °C and completing at 360 °C. Then the anhydrous complex suffered from serious mass loss upon heating to 400 °C, attributable to decomposition of the organic ligands. The Cu-*btc* loses all the organic ligands beginning from ca. 400 °C, so higher temperatures of 500 °C were chosen for the ideal thermal decomposition temperature for the Cu-*btc* MOF.

3.2. From the Cu-btc MOF to Cu 3D superstructures

In general, Cu nano- and microstructures can be synthesized in solution or solid state with the presence of chemical reducing agent [18–22]. However, the yield and purity of the Cu nano- and microstructures synthesized from solution is low, even in solid-state routes, where the formation rate increased with the increase of raw material. To the best of our knowledge, there is no report of one-step solid-state synthesis of Cu 3D superstructures even from coordination complexes. In this study, novel symmetrical coralloid Cu 3D superstructures with surface interspersed with clusters of Cu nanoparticles were simply synthesized by thermolysis of the Cu-*btc* MOF at 500 °C in the OCTF system without using any additional reducing agent or template.

The crystalline structures and phase purity of as-synthesized products were first examined by XRD with results shown in Fig. 2(a). The crystal structure of these products by thermolysis of the Cu-*btc* MOF in the OCTF at 500 °C for 10 h is confirmed to be copper phase (Sys: cubic; lattice: face-centered; S.G.: *Fm*3*m* (225); cell parameters: $a = 3.615$ Å; JCPDS file no. 04-0836) and the four diffraction peaks are well-matched to (111), (200), (220), (311), and (222) crystal faces of pure solid copper phase. No peaks of other phases can be found, indicating that pure products were obtained. Furthermore, EDX spectrum in Fig. 2(b) demonstrates that only Cu and Au elements appeared, indicating pure phase Cu was obtained by our approach and Au came from the sprinkled Au for SEM examination of the samples.

The morphology and sizes of as-synthesized Cu products were further characterized by SEM. As can be seen from a typical low magnification FE-SEM image in Fig. 3(a), large-scale Cu products

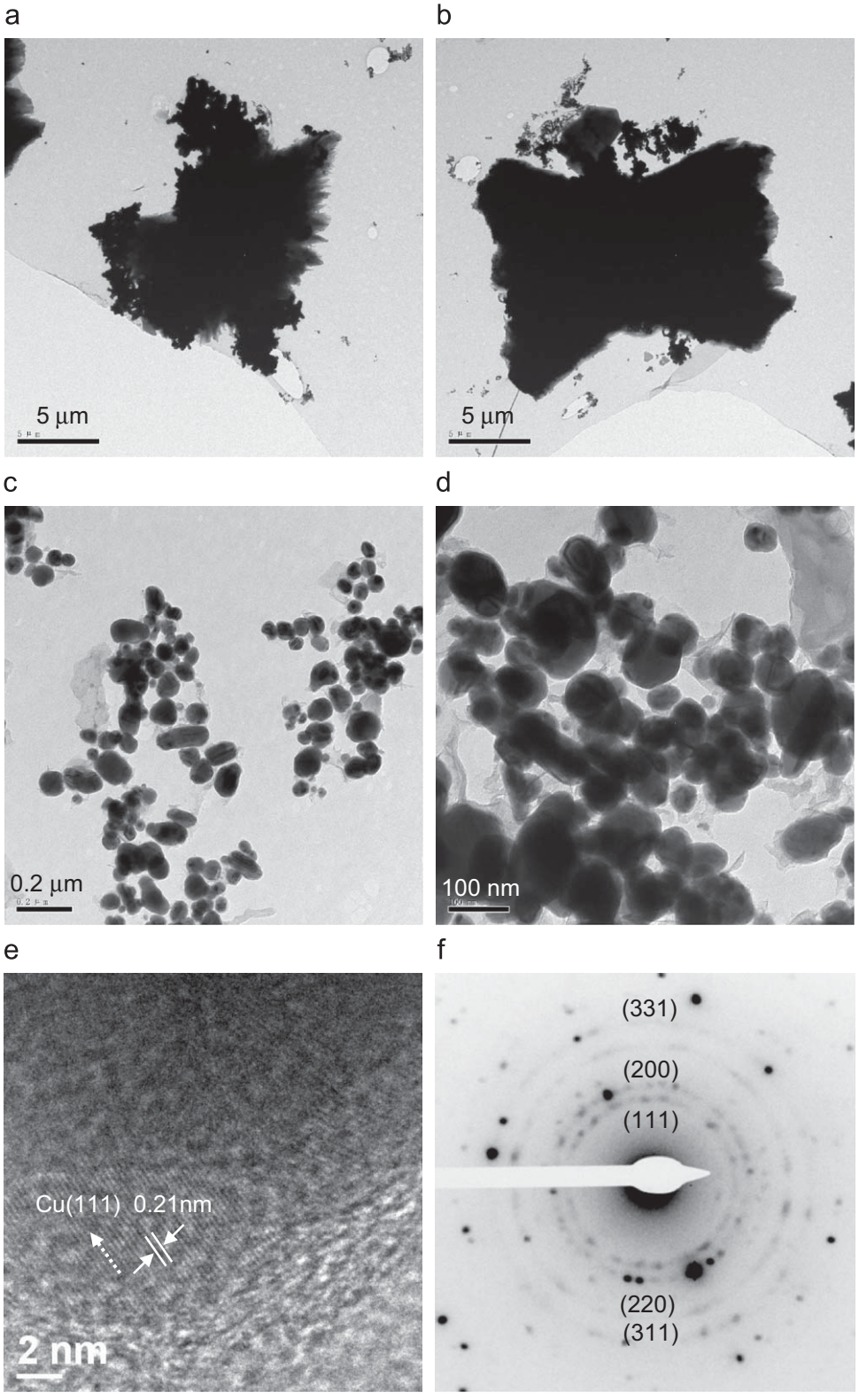

Fig. 4. (a), (b) Typical TEM images of as-synthesized single Cu superstructure by thermolysis of the Cu-*btc* MOF in the OCTF at 500 °C for 10 h, and (c) and (d) TEM images, (e) a HRTEM image, and (f) a SAED image of the formed Cu nanoparticles on the surface of as-synthesized Cu superstructures.

were obtained by our approach. As shown in Fig. 3(b) and (c), the synthesized Cu microstructures exhibit beautiful and coralloid structures (see a typical photography of one kind of corals in Fig. 3(f)), with the diameter varying from 0.5 to 10 μm. And a lot of clusters of Cu nanoparticles appear around the sides and surfaces of the synthesized superstructures. Most interestingly, all the synthesized coralloid microstructures have symmetrical structures. Furthermore, Fig. 3(d) shows an urchin-like port of the synthesized

coralloid Cu microstructure. From the above analysis, three typical traits can be clearly seen as following: (I) the synthesized "coral" has obvious walls, (II) many small nanoparticles appeared on the surface and beside the as-synthesized "coral", and (III) the "coral" has symmetrical structures. Although understanding the formation mechanism is not easy, this is the first result of symmetrical coralloid and Cu superstructure.

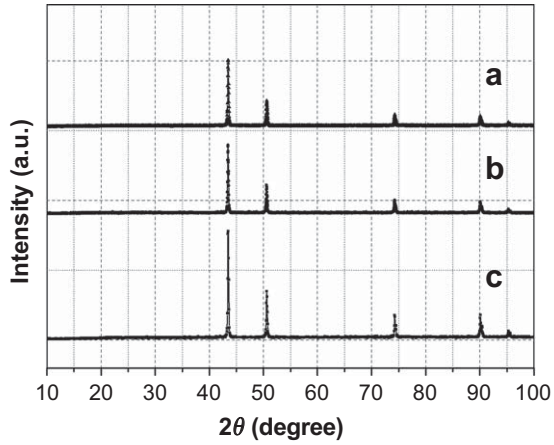

Fig. 5. Different XRD patterns of as-synthesized Cu products by thermolysis of the Cu-*btc* MOF in the OCTF at 500 °C for different reaction times of (a) 5 h, (b) 20 h, and (c) 30 h.

More detailed structure information on the synthesized Cu superstructures was investigated by TEM shown in Fig. 4(a) and (b), which further indicated the coralloid structure of a single coral with a size of about 10 μm. Clear surface structures of the single coral cannot be shown for its large scale. In order to examine the size, morphology, and composition of as-synthesized Cu nanoparticles on the surface and beside as-synthesized Cu superstructures by ultrasonic of the sample in ethanol for half an hour, further characterization was displayed by TEM. From different magnification TEM images in Fig. 4(c) and (d), the synthesized Cu nanoparticles have a diameter varying from 50 to 80 nm. The HRTEM image in Fig. 4(e) and SEAD image in Fig. 4(f) further indicate that the synthesized nanoparticles are pure phase Cu products. Fig. 4(e) shows a typical HRTEM image of an individual Cu nanoparticle, giving resolved lattice fringes of (111) planes ($d_{111} = 0.21$ nm). The SAED pattern in Fig. 4(f) taken from a single Cu nanoparticle indicates that Cu has cubic structure with space group $Fm3m$ (225) and lattice constant $a = 3.615$ Å [20,45].

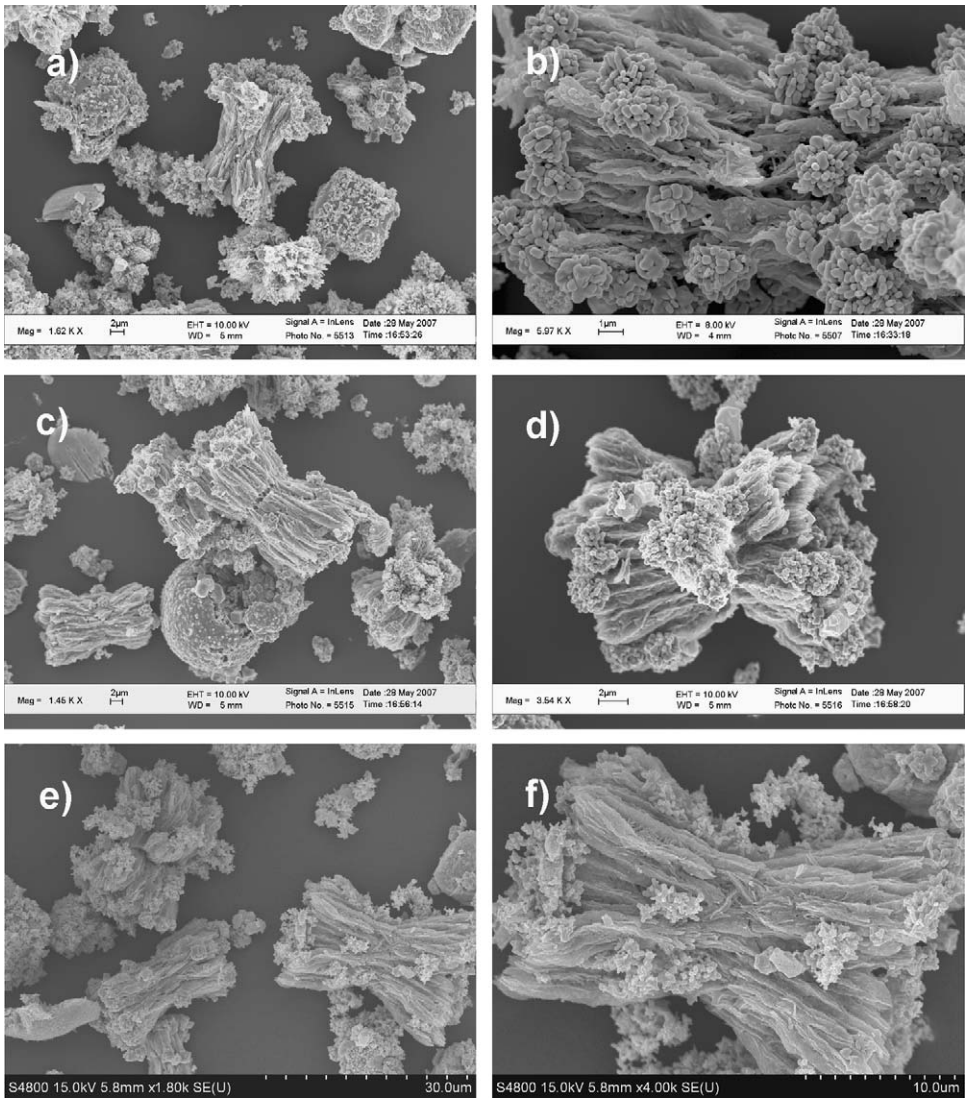

Fig. 6. Different magnification FE-SEM images of the Cu microstructures by thermolysis of the Cu-*btc* MOF in the OCTF at 500 °C for different reaction times of (a) and (b) 5 h, (c) and (d) 20 h, and (e) and (f) 30 h.

3.3. Reaction conditions on the final products

Reaction conditions have a large effect on the final products (in Table 1). When the Cu-*btc* MOF was calcinated at 500 °C for 10 h in the air, only irregular CuO microstructures were obtained with the FE-SEM image and XRD patterns in Fig. S2. To investigate the role of reaction time on the final products during thermolysis of the Cu-*btc* MOF in the OCTF system, we further studied the morphology of the final products by thermolysis of the Cu-*btc* MOF at 500 °C for different reaction time varying from 5 and 10 h to 20 and 30 h. Fig. 5 shows XRD patterns of the synthesized CuO by thermolysis of the Cu-*btc* at 500 °C for different reaction times of 5, 20, and 30 h, indicating that pure Cu products were obtained. From Fig. 6(a) and (b) it can be seen that shorter coralloid Cu microstructures and a lot of Cu nanoparticles formed at 500 °C for 5 h. With the increase of reaction time to 10 h, more and longer coralloid Cu microstructures with diameter of about 12 μm appeared and there were still large amount of clusters composed by Cu nanoparticle displayed on the surface and beside the synthesized superstructures (in Fig. 3). When the reaction time was increased to 20 and 30 h, uninformed and larger coralloid microstructures were obtained with length of about 15 and 20 μm and width of 5 and 10 μm (in Fig. 6(e) and (f)). From this, we can see that with the increase of reaction time, coralloid Cu microstructures can be obtained, but with the increase in diameter still large amount of Cu nanoparticles appeared on the surface and beside these synthesized Cu superstructures.

Table 1
The effect of reaction conditions on the shapes of the final products.

	Thermolysis means	*T* (°C)	*t* (h)	Shape
1	A	500	5	Coralloid
2	A	500	10	Coralloid
3	A	500	20	Coralloid
4	A	500	30	Coralloid
5	B	500	5	Coralloid
6	B	500	10	Coralloid
7	C	500	10	Irregular

(A) Thermolysis in the OCTF, (B) heating of the synthesized Cu superstructures in the air, and (C) direct calcination of the Cu-btc in the air.

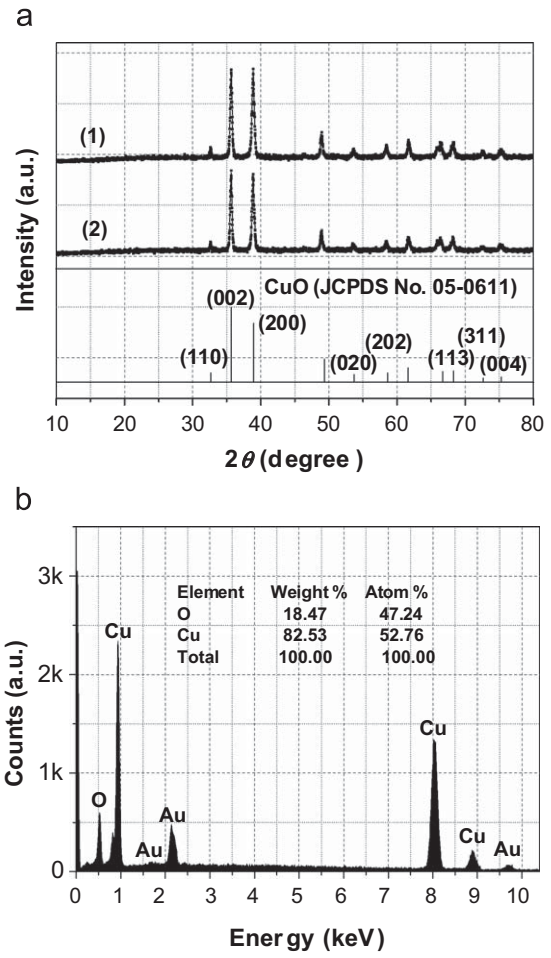

Fig. 7. (a) XRD patterns of as-synthesized Cu products by in-situ calcinations of Cu superstructures (obtained by thermolysis of the Cu-*btc* in the OCTF at 500 °C for 10 h) at 500 °C for the reaction time of (1) 5 h and (2) 10 h in the air and (b) EDX spectrum of as-synthesized products by calcinations of Cu superstructures at 500 °C for 10 h in the air.

3.4. From Cu superstructures to CuO superstructures

Material conversion is one of the important research fields [46]. Novel CuO microstructures were obtained by in-situ calcination of as-synthesized Cu superstructures in the air. Fig. 7(a) and (b) show XRD patterns of as-synthesized products by in-situ calcination of the as-synthesized Cu superstructures (obtained by thermolysis of the Cu-*btc* MOF in the OCTF at 500 °C for 10 h) in the air at 500 °C for 5 and 10 h. Both of the two products were CuO. The EDX spectrum in Fig. 7(c) further indicated that pure CuO products were obtained by in-situ thermal conversion. After calcination, coralloid morphology of the products still existed and their sizes became bigger (see FE-SEM images in Fig. 8). The former Cu nanoparticles turned into bigger spheres and nanoparticle-clusters into sphere-clusters. More information on the synthesized single CuO microspheres were investigated by magnified FE-SEM shown in Fig. 8(c) and (d) which showed regular spherical microstructures. From TEM images in Fig. 8(e) and (f) it can be seen that the formed CuO microparticles have a diameter of about 200 nm. By direct heating of the above synthesized Cu microstructures, we realized the conversion from Cu to CuO in-situ and morphology remained unchanged.

3.5. Possible formation mechanism

In general, thermolysis of the metal-organic frameworks results in metal oxide products. Very recently, metal oxide nanostructures such as ZnO nanoparticles [32,47,48] and CdO nanowires [49] were synthesized by direct thermolysis of corresponding metal-organic frameworks in the air. With the temperature increase, the precursor decomposed its organic ligands and at higher temperature the ligands decomposed into carbon and different kinds of gases including hydrogen, carbon monoxide, and benzene, together with other fragments from the incomplete decomposed ligands [33,38,50] which have strong reducibility. The formation process of thermolysis of the Cu-*btc* MOF precursor into Cu nano- and microstructures is essentially composed of decomposition, reduction, nucleation, and growth. Finally, the decomposed Cu formed symmetrical coralloid superstructures in the reductive environment. Further mechanism research in detail is under exploration.

4. Conclusions

In conclusion, we have demonstrated the successful synthesis of symmetrical coralloid Cu 3D superstructures with surface interspersed with clusters of Cu nanoparticles by one-step solid-

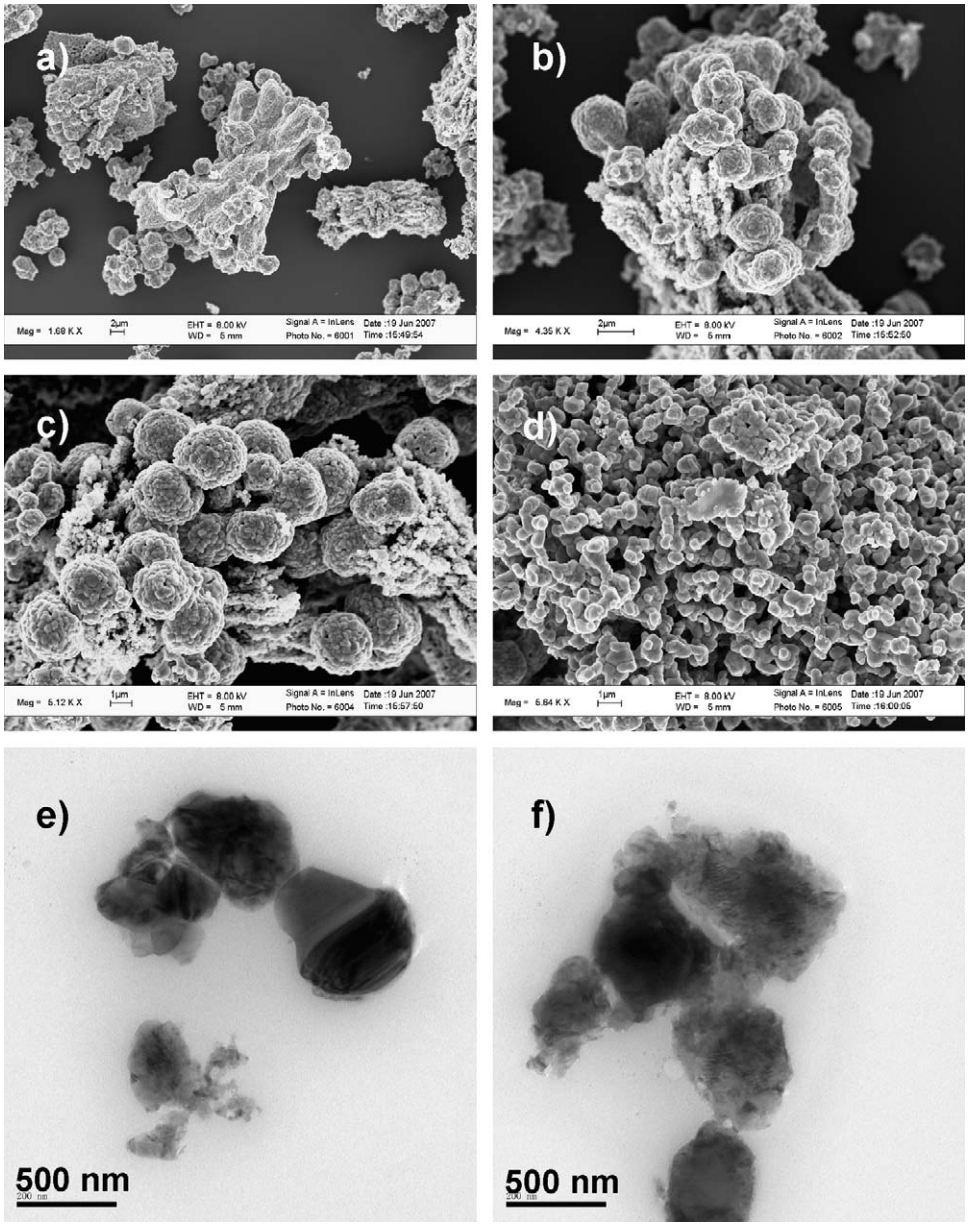

Fig. 8. (a), (b) Low magnification FE-SEM images, (c), (d) high magnification FE-SEM images, and (e), (f) TEM images of as-synthesized Cu products by in-situ calcinations of Cu superstructures (obtained by thermolysis of the Cu-*btc* in the OCTF at 500 °C for 10 h) at 500 °C for 10 h in the air.

state thermolysis of the Cu-*btc* MOF in the OCTF system. For the first time, direct solid-state transformation of Cu-*btc* MOF into coralloid Cu 3D superstructures was realized with the strategy of the decomposed organic component affecting the remaining inorganic components. Thermolysis temperature and reaction time have a large effect on the sizes and shapes of the final products. Furthermore, novel CuO superstructures were also obtained by in-situ thermal calcination of the as-synthesized coralloid Cu 3D superstructures in the air. Compared with the reported methods for the synthesis of Cu and CuO, the advantage of this synthetic route lies in its simplicity including easy synthesis, environmental friendliness with use of a benign precursor, relatively low temperature, and high yield of Cu product, as well as without using any additional reductive, surfactant, or template. This process also builds a direct linkage between metal-carboxylate MOF crystals and metal nano- or microstructures and further opens a new application field of MOFs.

Acknowledgments

We thank Prof. Xiaoheng Liu (Nanjing University of Science and Technology) for HRTEM measurements. This work was financially supported by the National Natural Science Foundation of China (no. 20771058), the Major State Basic Research Development Program (Grant no. 2006CB86104), and the NSFC Fund for Creative Research Groups (no. 20721002). We also thank the Scientific Research Foundation for Talent Introduction of Chongqing University.

Appendix A. Supplementary material

Supplementary data associated with this article can be found in the online version at doi:10.1016/j.jssc.2009.06.007.

References

[1] B. Bhushan, Springer Handbook of Nanotechnology, Springer, Berlin, Heidelberg, New York, 2007.
[2] Q. Zhang, S.J. Liu, S.H. Yu, J. Mater. Chem. 19 (2009) 191.
[3] C.N.R. Rao, A. Müller, A.K. Cheetham, Nanomaterials Chemistry: Recent Developments and New Directions, Wiley-VCH, 2007.
[4] Wang, J. Mater. Chem. 15 (2005) 1021.
[5] S.H. Sun, H. Zeng, D.B. Robinson, S. Raoux, P.M. Rice, S.X. Wang, G.X. Li, J. Am. Chem. Soc. 1236 (2004) 273.
[6] S.L. Brock, K. Senevirathne, J. Solid State Chem. 181 (2008) 1552.
[7] X. Wang, J. Song, J. Liu, Z. Wang, Science 316 (2007) 102.Z.
[8] X. Zhang, C. Sui, J. Gong, Z. Su, L. Qu, J. Phys. Chem. C 111 (2007) 9049.
[9] K.J. Ziegler, R.C. Doty, K.P. Johnston, B.A. Korgel, J. Am. Chem. Soc. 125 (2003) 16050.
[10] Z. Liu, Y. Yang, J. Liang, Z. Hu, S. Li, S. Peng, Y. Qian, J. Phys. Chem. B 107 (2003) 12658.
[11] R.M. Erb, H.S. Son, B. Samanta, V.M. Rotello, B.B. Yellen, Nature 457 (2009) 999.
[12] M.K. Wu, J.R. Ashburn, C.J. Torng, P.H. Hor, R.L. Meng, L. GaoZ.J. Huang, Y.Q. Wang, C.W. Chu, Phys. Rev. Lett. 58 (1987) 908.
[13] J.B. Reitz, E.I. Solomon, J. Am. Chem. Soc. 120 (1998) 11467.
[14] K.J. Ziegler, R.C. Doty, K.P. Johnston, B.A. Korgel, J. Am. Chem. Soc. 20 (2001) 5109.
[15] Z. Liu, Y. Yang, J. Liang, Z. Hu, S. Li, S. Peng, Y. Qian, J. Phys. Chem. B 107 (2003) 12658.
[16] M.K. Wu, J.R. Ashburn, C.J. Torng, P.H. Hor, R.L. Meng, L. Gaoet al., Phys. Rev. Lett. 58 (1987) 908.
[17] J.B. Reitz, E.I. Solomon, J. Am. Chem. Soc. 120 (1998) 11467.
[18] A.O. Musa, T. Akomolafe, M.J. Carter, Sol. Energy Mater. Sol. Cell 51 (1998) 305.
[19] B. Liu, H.C. Zeng, J. Am. Chem. Soc. 126 (2004) 8124.
[20] Y. Liu, Y. Chu, Y. Zhuo, L. Dong, L. Li, M. Li, Adv. Funct. Mater. 17 (2007) 933.
[21] C. Salzemann, A. Brioude, M. Pileni, J. Phys. Chem. B 110 (2006) 7208.
[22] M. Cao, C. Hu, Y. Wang, Y. Wang, Y. Guo, C. Guo, E. Wang, Chem. Commun. 6 (2003) 1884.
[23] Y. Xu, D. Chen, X. Jiao, J. Phys. Chem. B 109 (2005) 13561.
[24] J.L.C. Rowsell, E.C. Spencer, J. Eckert, J.A.K. Howard, O.M. Yaghi, Science 309 (2005) 1351.
[25] G. Férey, C. Mellot-Draznieks, C. Serre, F. Millange, J. Dutour, S. Surblé, I. Margiolaki, Science 309 (2005) 2040.
[26] C.D. Wu, A.G. Hu, L. Zhang, W.B. Lin, J. Am. Chem. Soc. 127 (2005) 8940.
[27] J.Y. Lee, D.H. Olson, L. Pan, T.J. Emge, J. Li, Adv. Funct. Mater. 17 (2007) 1255.
[28] L.G. Qiu, L.N. Gu, G. Hu, L.D. Zhang, J. Solid State Chem. 182 (2009) 502.
[29] J.J. Vittal, M.T. Ng, Acc. Chem. Res. 39 (2006) 869.
[30] S. Jung, W. Cho, H.J. Lee, M. Oh, Angew. Chem. Int. Ed. 48 (2009) 1459.
[31] J. Hambrock, S. Rabe, K. Merz, A. Birkner, A. Wohlfart, R.A. Fischer, et al., J. Mater. Chem. 13 (2003) 1733.
[32] H. Thakuria, G. Das, Polyhedron 26 (2007) 149.
[33] W. Schmitt, J.P. Hill, S. Malik, C.A. Volkert, I. Ichinose, C.E. Anson, et al., Angew. Chem. Int. Ed. 44 (2005) 7048.
[34] S.N. Wang, H. Xing, Y.Z. Li, J.F. Bai, Y. Pan, M. Scheer, et al., Eur. J. Iorg. Chem. (2006) 3041.
[35] S.N. Wang, H. Xing, Y.Z. Li, J.F. Bai, M. Scheer, Y. Pan, et al., Chem. Commun. 10 (2007) 2293.
[36] S.N. Wang, H. Xing, Y.Z. Li, J. Bai, M. Scheer, Y. Pan, et al., Chem. Commun. 10 (2007) 4416.
[37] R. Sun, S.N. Wang, H. Xing, J.F. Bai, Y.Z. Li, Y. Pan, et al., Inorg. Chem. 46 (2007) 8451.
[38] L.Y. Chen, J.F. Bai, C.Z. Wang, Y. Pan, M. Scheer, X.Z. You, Chem. Commun. 11 (2008) 1581.
[39] L.Y. Chen, H. Xing, Y.M. Shen, J.F. Bai, J. Solid State Chem. 182 (2009) 1387.
[40] Q.M. Wang, D. Shen, M. Bülow, M.L. Lau, S. Deng, F.R. Fitch, N.O. Lemcoff, J. Semanscin, Microporous Mesoporous Mater. 55 (2002) 217.
[41] K. Schlichte, T. Kratzke, S. Kaskel, Microporous Mesoporous Mater. 73 (2004) 81.
[42] P. Krawiec, M. Kramer, M. Sabo, R. Kunschke, H. Fröde, S. Kaskel, Adv. Eng. Mater. 8 (2006) 293.
[43] E. Biemmi, C. Scherb, T. Bein, J. Am. Chem. Soc. 129 (2007) 8054.
[44] D. Zacher, A. Baunemann, S. Hermes, R.A. Fischer, J. Mater. Chem. 17 (2007) 2787.
[45] Z.L. Wang, X.Y. Kong, X.G. Wen, S.H. Yang, J. Phys. Chem. 107 (2003) 8275.
[46] Y. Vasquez, A.E. Henkes, J.C. Bauer, R.E. Schaak, J. Solid State Chem. 181 (2008) 1509.
[47] C.Y. Su, A.M. Goforth, M.D. Smith, P.J. Pellechia, H.C. Zur Loye, J. Am. Chem. Soc. 126 (2004) 3576.
[48] H. Thakuria, B.M. Borah, G. Das, Eur. J. Inorg. Chem. (2007) 524.
[49] F. Zhang, F.L. Bai, J.M. Cao, X. Wang, J. Solid State Chem. 181 (2008) 143.
[50] D.C.K. Lin, J.B. Westmore, Can. J. Chem. 51 (1973) 2999.